

# Sputtering of amorphous ice induced by $C_{60}$ and $Au_3$ clusters

Michael F. Russo Jr.<sup>\*</sup>, Igor A. Wojciechowski, Barbara J. Garrison

*Department of Chemistry, Penn State University, 104 Chemistry Building, University Park, PA 16802, United States*

Received 12 September 2005; accepted 15 February 2006

Available online 2 May 2006

## Abstract

Molecular dynamics simulations were performed to study the behavior of cluster SIMS. Two predominant cluster ion beam sources,  $C_{60}$  and  $Au_3$ , were chosen for comparison. An amorphous water ice substrate was bombarded with incident energy of 5 keV. The  $C_{60}$  cluster was observed to shatter upon impact creating a crater of damage approximately 8 nm deep. Although  $Au_3$  was also found to both break apart and form a damage crater, it continued along its initial trajectory causing damage roughly 10 nm deep into the sample and becoming completely imbedded. It is suggested that this difference in behavior is due to the large mass of Au relative to the substrate water molecule.

© 2006 Elsevier B.V. All rights reserved.

*Keywords:* Molecular dynamics; Cluster ion;  $Au_3$ ;  $C_{60}$

## 1. Introduction

In a matter of only a few years, the use of cluster ion beams has become a staple of the SIMS community as elucidated in a recent review article [1] and by the vast number of presentations at this conference, SIMS XV. This is due in large part to the many benefits clusters have to offer, which include yield enhancement, reduced substrate damage and the ability in certain cases to perform molecular depth profiling. Although a number of different cluster sources have been used over the years starting with  $SF_6^-$  [2], the two predominant commercial sources are now  $C_{60}^+$  and  $Au_3^+$  [3,4].

The differences in the two cluster beam sources are beginning to be explored in experiment. From a computational viewpoint, the predominant studies have been for metal substrates [5–8] or thin condensed films on a metal substrate [9–12]. Many of the current substrates of interest, however, are materials composed of lighter elements. Using the strategy for modeling the bombardment of an amorphous water ice from previous works [13,14] molecular dynamics simulations are performed in which the water ice substrate is bombarded with either  $Au_3$  or  $C_{60}$ . Through this comparative study, several aspects of sputtering are considered in order to yield clues as to the dynamic behavior of this event. These include the penetration depth of incident

particle, damage shape and depth, and path of the incident particle's constituents upon impact.

## 2. Computation details

The MD scheme utilized in these experiments has been explained elsewhere [15,16]. Simulations were performed using amorphous water ice as the substrate. In the case of the  $C_{60}$  bombardment, a sample consisting of 1.21 million atoms: 400,000 water molecules, and  $\sim 3000$  Na and Cl ions, was arranged to be 29.3 nm  $\times$  29.3 nm  $\times$  16.1 nm and equilibrated to  $\sim 300$  K with rigid and stochastic layers employed on the edges to prevent the reflection of pressure waves [17]. The same crystal was then reoriented and trimmed down to accommodate the expected deeper implantation of the  $Au_3$ . This substrate measured 16.0 nm  $\times$  16.0 nm  $\times$  32.5 nm with 242,000 water molecules, and  $\sim 2000$  Na and Cl ions for a total of 730,000 atoms. As a side note, although our primary focus is on the impact dynamics, the Na and Cl were added so that we could also study ion effects which will be discussed at a later time.

The forces between atoms within the substrate were described by a mix of several different empirical pair-wise additive potential functions with water molecules constrained to be rigid through the use of the RATTLE algorithm. The descriptions of these potentials along with their parameters have been described elsewhere [13,14]. For the incident clusters all interactions with substrate constituents were modeled using

<sup>\*</sup> Corresponding author.

*E-mail address:* [mfr129@psu.edu](mailto:mfr129@psu.edu) (M.F. Russo Jr.).

a Moliere potential. With Au–Au, we employed a Molecular Dynamics/Monte Carlo Corrected Effective Medium potential (MD/MC-CEM) [21] and for C–C we made use of the AIREBO potential [22] which was adapted from the REBO potential for hydrocarbons developed by Brenner [23,24].

Both projectiles were given 5 keV of initial energy and directed at the substrate normal to the surface. The atoms within the incident particles were given initial velocities of zero relative to their center of mass and their orientation was determined randomly. One trajectory was performed for both systems and each is currently discussed up to 5 ps.

### 3. Results

Representative cross section views at different times are shown in Fig. 1 for each projectile. They represent a 2.0 nm thick slice of the sample centered on the point of impact. While it is

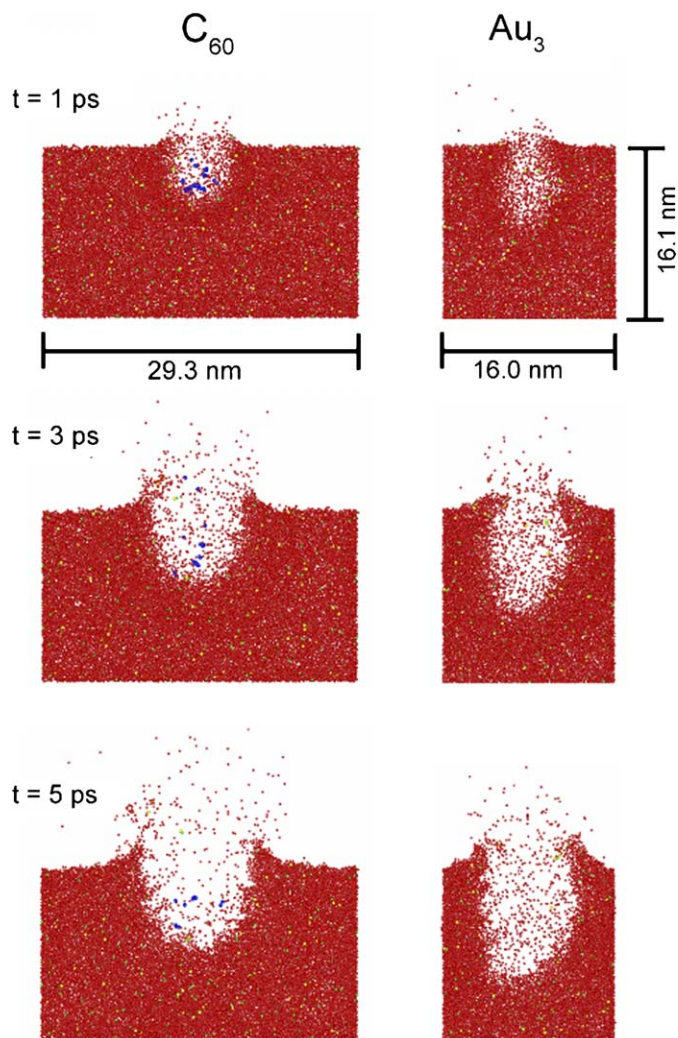


Fig. 1. A 2.0 nm thick slab cut through the center of the crystal is shown at three intermediate times to provide a cross sectional view of the collision event using 5 keV  $C_{60}$  and  $Au_3$  as projectiles. Red, yellow, and green represent oxygen, sodium, and chlorine atoms, respectively. Blue represents the incident particles. Hydrogen is present but not shown for simplicity. *Note:*  $Au_3$  substrate truncated. (For interpretation of the references to color in this figure legend, the reader is referred to the web version of the article.)

clear that the  $C_{60}$  bombardment follows the similar dynamics as reported in the past [17,25], there are several obvious differences when compared to the  $Au_3$ . In the first image at 1 ps the  $C_{60}$  projectile breaks apart upon contact with the substrate creating a spherical crater region and initiating a spherical pressure wave. In comparison to earlier substrates of silver, the amorphous ice is much lighter in mass and less weakly bound. As a result none of the carbon atoms are immediately backscattered due to reflection as was seen previously [17,25]. The Au atoms with a mass 10 times that of  $H_2O$  meet little resistance from the water, thus traveling deep into the sample and beginning the formation of a cylindrical crater and pressure wave. Fig. 2a and b illustrate the motion of each incident cluster particle leading up to the 1 ps snapshot. Each sequence is comprised of 25 still frame images, taken at 40 fs intervals for each of the clusters and colored by time. Between 80 and 120 fs (third and fourth sets of positions) it is apparent that the  $C_{60}$  has collapsed while the  $Au_3$  begins to drift apart but remain correlated in its downward motion. By the end of the sequence, the gold has slowed to rest at approximately a depth of 10 nm, while the carbon atoms continue to have random motion within the lower edge of the damage crater roughly 4.5 nm deep. From the yellow and red positions near the end of

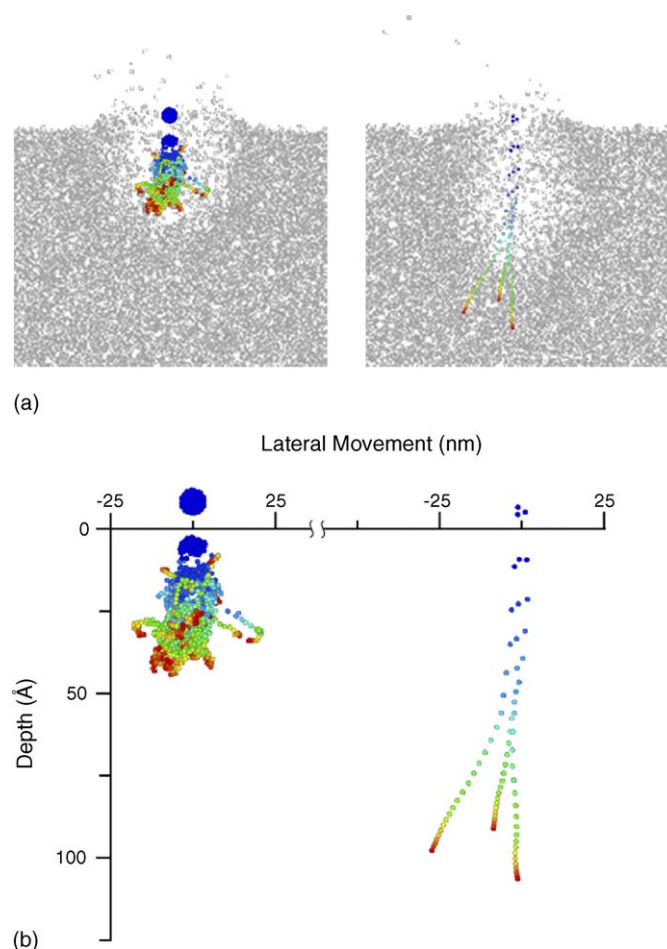


Fig. 2. (a) Time lapse image of the  $C_{60}$  and  $Au_3$  over their respective substrates. Colors represent different frames with 40 fs between each. (b) Close up of time lapse images with depth and lateral motion of the incident cluster for comparison.

the sequence, a few of the carbons can be seen moving toward the surface.

By 3 ps the pressure wave generated by both clusters has begun to create a hole in the sample surface and force the removal of material around its epicenter. The dimensions of both craters have increased to roughly double what they were at the 1 ps mark. Finally, after 5 ps the damage has expanded further in both samples as the damage craters are approaching 10.1 nm wide  $\times$  7.6 nm deep for the C<sub>60</sub> and 8.0 nm wide  $\times$  9.9 nm deep for the Au<sub>3</sub>.

#### 4. Conclusions

The MD simulations presented provide a picture of the important differences between clusters of similar total mass but different mass of their individual particles. Interestingly, even though the initial dynamics of each crater's formation are quite different, there is only a slight distinction between their final shapes and sizes. These images suggest that the primary difference between these two events is the implantation of Au, which is proposed to be due to the 20 times larger mass of gold over carbon. The larger mismatch of mass between the Au and the substrate water molecules allows the incident cluster atoms to retain much of their initial energy and travel deep into the sample relatively unhindered. This observed behavior of Au implantation supports experimental findings suggesting a build up of gold due to increased Au<sub>3</sub> signal with successive bombardments [26]. The C<sub>60</sub> consists of many more particles, which upon impact dissociate in all directions, dissipating their initial energy in the very near surface region. This rapid transfer of energy prohibits the effective embedding of carbon into the sample. Although predominantly qualitative at this stage, these calculations illustrate some the key differences in behavior of the C<sub>60</sub> and Au<sub>3</sub> projectiles and necessitate further study into the dynamic process of cluster SIMS.

#### Acknowledgements

The authors would like to thank the Chemistry Division of the National Science Foundation for financial support of this

work. Special thanks also to Professor Zbigniew Postawa for his insight and helpful discussions.

#### References

- [1] N. Winograd, *Anal. Chem.* 77 (2005) 142A.
- [2] A.D. Appelhans, J.E. Delmore, *Anal. Chem.* 61 (1989) 1087.
- [3] N. Davies, D.E. Weibel, P. Blenkinsopp, N. Lockyer, R. Hill, J.C. Vickerman, *Appl. Surf. Sci.* 203 (2003) 223.
- [4] S.C.C. Wong, R. Hill, P. Blenkinsopp, N.P. Lockyer, D.E. Weibel, J.C. Vickerman, *Appl. Surf. Sci.* 203 (2003) 219.
- [5] H.M. Urbassek, C. Anders, *Nucl. Instrum. Methods Phys. Rec. Sect. B* 228 (2004) 57.
- [6] H.M. Urbassek, C. Anders, *Nucl. Instrum. Methods Phys. Rec. Sect. B* 228 (2004) 84.
- [7] H.M. Urbassek, C. Anders, *Phys. Rev. B* 70 (2004).
- [8] H.M. Urbassek, S. Zimmermann, *Nucl. Instrum. Methods Phys. Rec. Sect. B* 228 (2004) 75.
- [9] Z. Postawa, *Appl. Surf. Sci.* 231-2 (2004) 22.
- [10] Z. Postawa, B. Czerwinski, N. Winograd, B.J. Garrison, *J. Phys. Chem. B* 109 (2005) 11973.
- [11] Z. Postawa, K. Ludwig, J. Piaskowy, K. Krantzman, N. Winograd, B.J. Garrison, *Nucl. Instrum. Methods Phys. Res. Sect. B* 202 (2003) 168.
- [12] Z. Postawa, C.A. Meserole, P. Cyganik, J. Szymonska, N. Winograd, *Nucl. Instrum. Methods Phys. Res. Sect. B* 182 (2001) 148.
- [13] I. Wojciechowski, S.X. Sun, C. Szakal, N. Winograd, B.J. Garrison, *J. Phys. Chem. A* 108 (2004) 2993.
- [14] I.A. Wojciechowski, U. Kutliev, S.X. Sun, C. Szakal, N. Winograd, B.J. Garrison, *Appl. Surf. Sci.* 231-2 (2004) 72.
- [15] B.J. Garrison, *Chem. Soc. Rev.* 21 (1992) 155.
- [16] B.J. Garrison, Molecular dynamics simulations, the theoretical partner to static SIMS experiments, in: J.C. Vickerman, D. Briggs (Eds.), *ToF-SIMS: Surface Analysis by Mass Spectrometry, Surface Spectra*, Manchester, 2001, p. 223.
- [17] Z. Postawa, B. Czerwinski, M. Szewczyk, E.J. Smiley, N. Winograd, B.J. Garrison, *Anal. Chem.* 75 (2003) 4402.
- [21] C.L. Kelchner, D.M. Halstead, L.S. Perkins, N.M. Wallace, A.E. DePristo, *Surf. Sci.* 310 (1994) 425.
- [22] S.J. Stuart, A.B. Tutein, J.A. Harrison, *J. Chem. Phys.* 112 (2000) 6472.
- [23] D.W. Brenner, *Phys. Rev. B* 42 (1990) 9458.
- [24] D.W. Brenner, O.A. Shenderova, J.A. Harrison, S.J. Stuart, B. Ni, S.B. Sinnott, *J. Phys. Condens. Matter* 14 (2002) 783.
- [25] Z. Postawa, B. Czerwinski, M. Szewczyk, E.J. Smiley, N. Winograd, B.J. Garrison, *J. Phys. Chem. B* 108 (2004) 7831.
- [26] J. Cheng, N. Winograd, unpublished results.